HAVSTOVAN
FAROE MARINE RESEARCH INSTITUTE

Observations from the WOW field experiment in the Western Valley 2016-2017

Data report

Tórshavn · August 2017

Bogi Hansen

Karin M. H. Larsen

Regin Kristiansen

Ebba Mortensen

Detlef Quadfasel

Kerstin Jochumsen

Svein Østerhus

HAVSTOVAN NR.: 17-03
TECHNICAL REPORT

The present project has been funded by the Danish Energy Agency as part of the Arctic Climate Support Programme. The authors are solely responsible for the results and conclusions presented in the report. They do not necessary reflect the position of the Danish Energy Agency.

Introduction

This data report documents the observations obtained during a 279 day long experiment with instruments deployed at three sites in the Western Valley on the Iceland-Faroe Ridge (Figure 1). The report is part of the "Western Valley Overflow" (WOW) project, which is a cooperation between the Faroe Marine Research Institute (Havstovan) and the Danish Meteorological Institute, funded by the Danish Energy Agency within the Danish Ministry of Energy, Utilities and Climate.

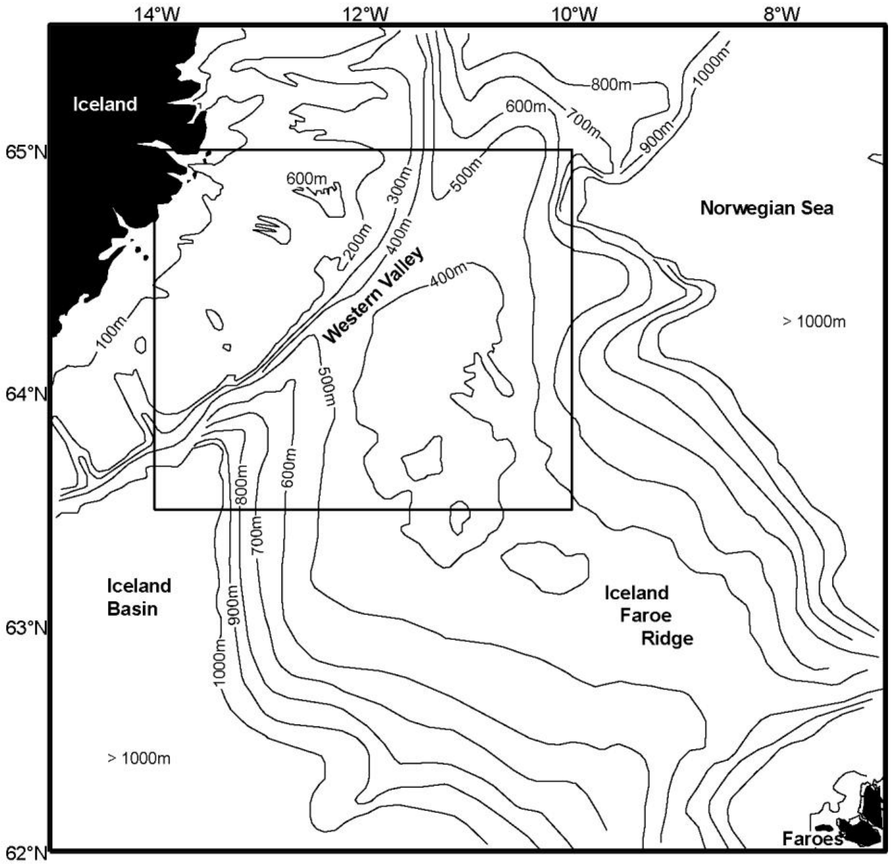

Figure 1. Bottom topography of the Iceland-Faroe Ridge showing the Western Valley and the selected area around it indicated by the rectangular box.

The Western Valley is the first deep passage across the ridge when following the ridge crest from the Icelandic to the Faroese end of the ridge. It has a sill depth around 400 m, which is considerably deeper than the typical upper boundary of dense water east of Iceland. Overflow of dense water would therefore be expected to pass through the valley and observations confirm that this does occur, but the evidence on its persistence has been ambiguous and no reliable estimates of the typical volume transport exist. This motivated the field experiment described in this report.

Table 1. Positions and depths of the three observational sites.

Site	Instruments	Latitude	Longitude	Depth
A	BTL	64°28.59'N	12°08.35'W	297m
B	ADCP+Microcat	64°26.70'N	12°03.76'W	402m
C	BTL	64°24.04'N	11°58.00'W	433m

The experiment

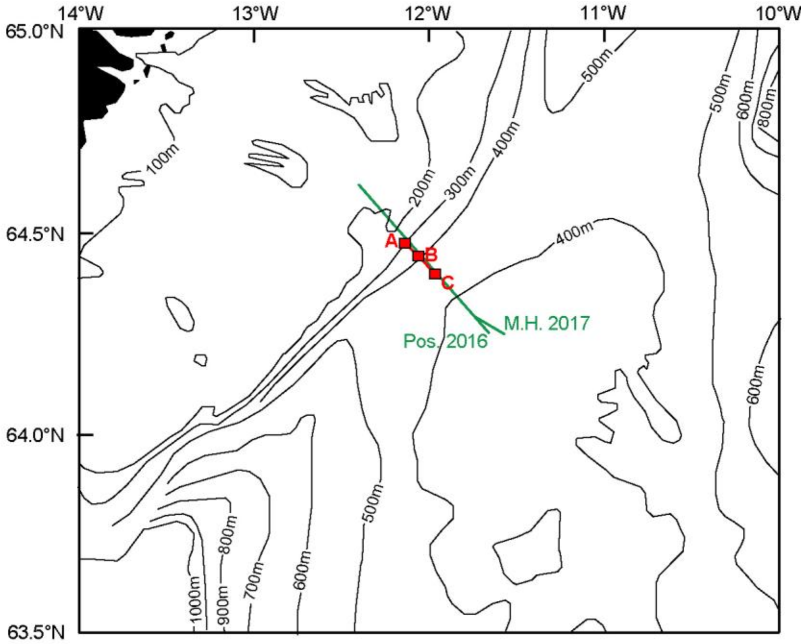

Figure 2. Bottom topography in the region of the Western Valley (rectangular box in Figure 1). Red squares indicate the three mooring sites of the field experiment. The green lines indicate CTD sections occupied by R/V Poseidon during the deployment cruise in 2016 (Pos. 2016) and by R/V Magnus Heinason during the recovery cruise in 2017 (M.H. 2017).

The three deployment sites were labelled A, B, and C (Figure 2). At sites A and C, each instrumental package contained a SeaBird SBE39 temperature recorder and battery packs attached to a LinkQuest acoustic modem enclosed in a specially developed trawl-protected frame (Figure 3, right panel) mounted on the bottom. Each of these "Bottom Temperature Loggers (BTL)" recorded the bottom temperature at hourly intervals.

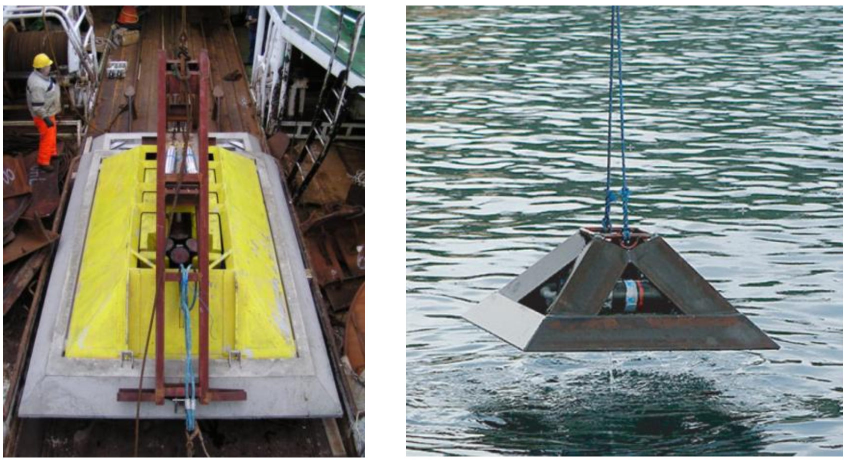

Figure 3. Left panel: An ADCP in a trawl-protective frame (yellow) onboard a research vessel, ready for deployment. Right panel: A bottom temperature logger (BTL) including temperature sensor, acoustic modem, and batteries in a trawl-protected frame.

At site B, a 150 kHz RDI Broadband ADCP (Acoustic Doppler Current Profiler) and a SeaBird Microcat (SBE37) were deployed within a trawl-protected frame (Figure 3, left panel) mounted on the bottom, which could be recovered by acoustic releases. The Microcat recorded bottom temperature, conductivity, and pressure at 10 minute intervals. The ADCP recorded velocity at 30 levels (bins) with 10m vertical resolution every 20 minutes. Originally, it had been planned to deploy two ADCPs in trawl-protected frames but, unfortunately, one of the instrumented frames, that was planned to be used, was lost in a previous deployment.

The instruments were deployed 14. August 2016 by R/V Poseidon. On 20. May 2017, R/V Magnus Heinason uploaded the bottom temperature measurements from the BTLs at sites A and C and recovered the ADCP and Microcat at site B. During both cruises, CTD stations were occupied along lines crossing the valley (Figure 4).

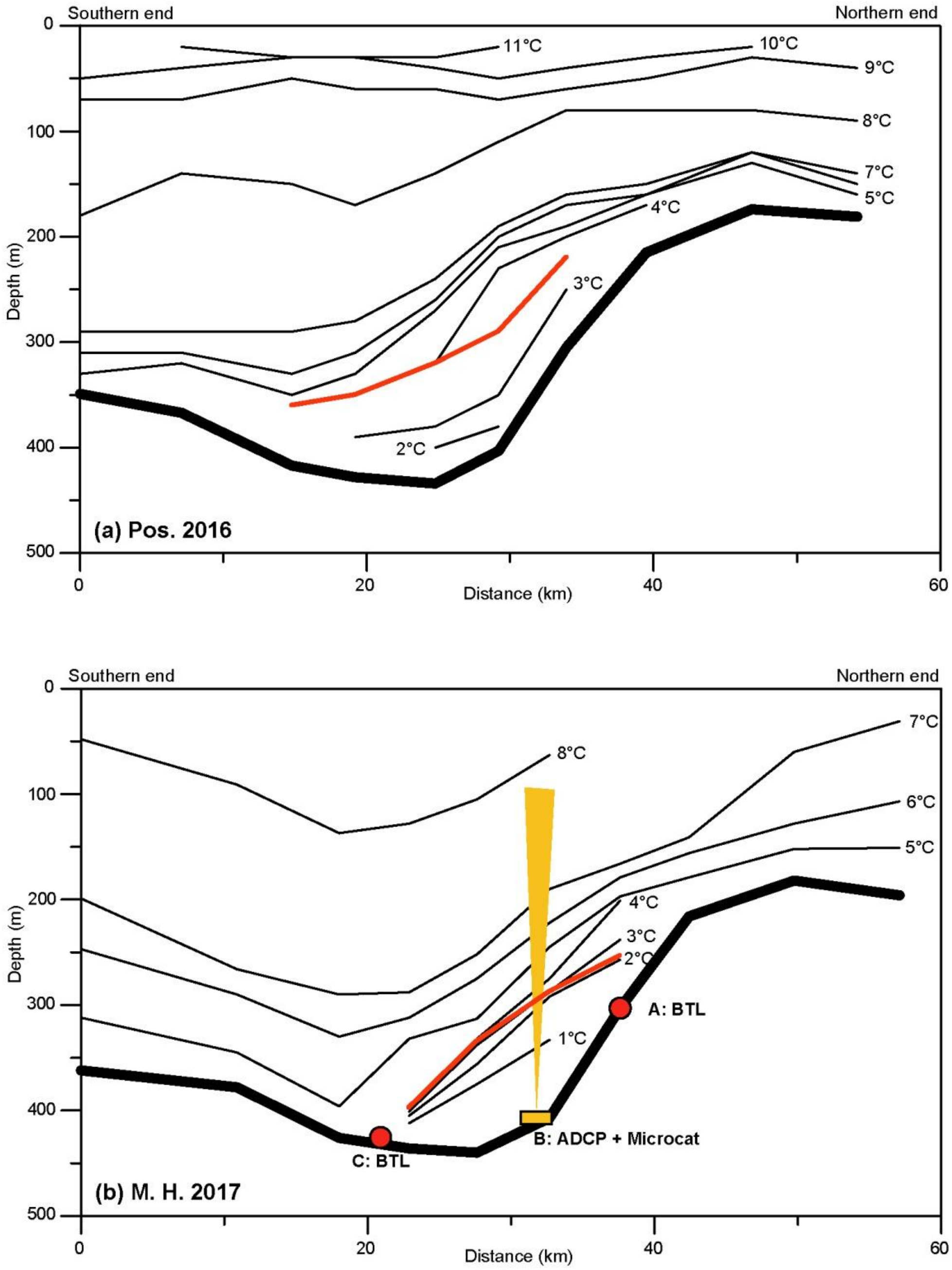

Figure 4. The temperature distribution on 17 August 2016 **(a)** as observed by R/V Poseidon and on 20 May 2017 **(b)** as observed by R/V Magnus Heinason. Section locations are indicated by the green lines in Figure 2. The thick red lines show the σ_θ = 27.8 kg m^{-3} isopycnal. The three moorings are indicated on **(b)** with the yellow cone representing the maximal ADCP range.

Data from moored instruments

All the temperature measurements from the deployed instruments were checked for data quality and appeared to be of high quality. The conductivity measurements of the Microcat showed spikes and a consistent drift through the observational period. They will not be further considered here.

The temperature measurements at the three sites were then converted to hourly intervals. The BTL temperatures were shifted to the nearest hour while hourly temperatures from the Microcat were calculated as averages of the 5 measurements from 20 minutes before to 20 minutes after the hour.

Histograms of the bottom temperatures (Figure 5) show that the ADCP site, site B, was almost always covered by water colder than 1°C, which can be characterized as overflow water. The other deep site, site C, had a bimodal temperature distribution indicating that it was sometimes in overflow water and sometimes in the warmer Atlantic water. At the shallowest site, site A, the bottom temperature was less than 10% of the time colder than 1°C. This indicates that the three sites were appropriately located with the ADCP site close to the core of the overflow and the two BTLs close to the boundaries of the overflow region as intended.

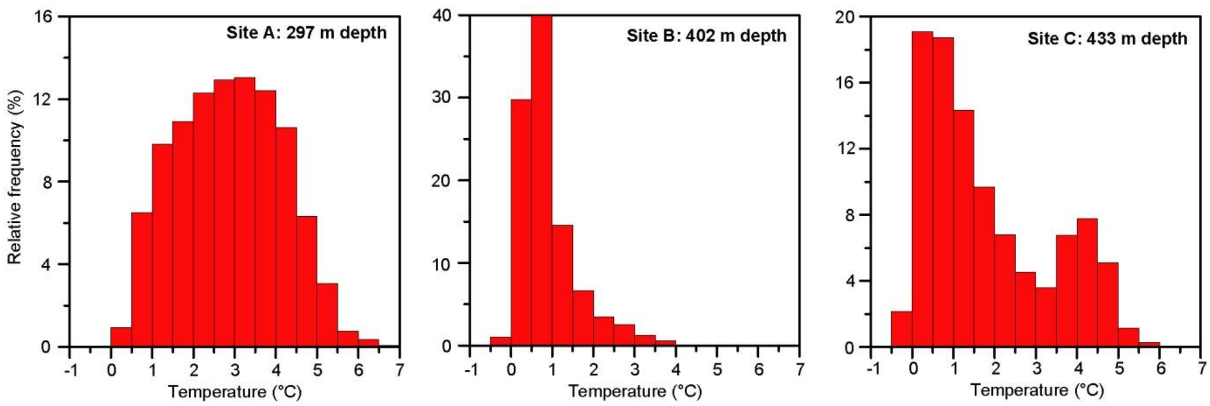

Figure 5. Histograms of bottom temperature at the three deployment sites based on hourly values.

The ADCP data have been quality controlled using a semi-automatic routine and erroneous data flagged (Table 2). The data have been processed such that threshold values for e.g. maximum error velocity, minimum mean correlation and others were set. Also, error velocities deviating more than a selected number of times the standard deviation from the mean error velocity were error flagged. Speed spikes are calculated in a similar manner selecting a number of standard deviations and then error flagging those values where u or v deviated more than the threshold from a 3 point median filtered u and v series. The velocity direction has been corrected for magnetic deviation. A frequency distribution of speeds for each bin is listed in Appendix A.

As for bottom temperature, the ADCP velocities were then averaged to hourly values. First, individual ensembles were interpolated vertically to reduce the number of flagged values. For each ensemble, flagged values of a single bin between two good bins were replaced by the average of the good bins. After that, the data were converted to hourly intervals by averaging the non-flagged ensembles from 20 minutes before to 20 minutes after the hour where the average for a bin was classified as good if at least two of the three ensembles were good for that bin.

Table 2. ADCP error statistics. For each bin are listed number of ensembles flagged (flgd) for intensity (Int.) and for velocity in number and % of total. For velocity is also shown the number of gaps of various lengths (gap length = number of consecutive flagged ensembles)

Bin	Int. ens. flgd	Velocity ens. flgd	% flgd	Number of velocity gaps of length									
				1	2	3	4	5	6-10	11-20	21-30	31-50	>50
1	0	94	0	76	9	0	0	0	0	0	0	0	0
2	0	132	1	104	11	2	0	0	0	0	0	0	0
3	0	172	1	146	8	2	1	0	0	0	0	0	0
4	0	179	1	155	12	0	0	0	0	0	0	0	0
5	0	196	1	161	13	3	0	0	0	0	0	0	0
6	0	199	1	165	17	0	0	0	0	0	0	0	0
7	0	244	1	185	28	1	0	0	0	0	0	0	0
8	0	266	1	209	22	3	1	0	0	0	0	0	0
9	0	273	1	197	31	2	2	0	0	0	0	0	0
10	0	282	1	207	30	2	1	1	0	0	0	0	0
11	0	290	1	201	36	4	0	1	0	0	0	0	0
12	0	300	1	224	29	6	0	0	0	0	0	0	0
13	0	337	2	245	32	5	2	1	0	0	0	0	0
14	0	359	2	228	50	6	2	1	0	0	0	0	0
15	0	371	2	240	38	10	5	1	0	0	0	0	0
16	0	424	2	261	58	9	3	0	1	0	0	0	0
17	0	524	3	285	63	11	5	2	3	2	0	0	0
18	0	641	3	296	76	15	6	6	4	3	1	0	0
19	0	728	4	274	67	12	6	5	13	6	2	0	0
20	0	887	4	248	92	12	4	2	10	8	4	3	0
21	0	1214	6	269	83	18	11	4	16	9	11	4	0
22	0	1524	8	267	67	19	11	4	23	14	12	9	0
23	0	2006	10	338	104	20	7	11	22	20	14	14	0
24	0	2494	12	376	108	32	11	7	17	28	14	24	0
25	0	3059	15	403	126	28	15	16	31	30	19	27	0
26	0	4154	21	477	143	57	29	15	46	52	22	34	1
27	0	5407	27	510	166	77	31	29	64	77	28	42	2
28	0	6963	35	492	168	72	47	33	79	92	44	59	3
29	0	8604	43	534	169	85	52	30	74	87	76	65	12
30	0	10252	51	567	188	80	65	32	76	71	94	78	21

The resulting data set contains 6700 values of hourly bottom temperature values at each of the three sites and 6700×30 values of hourly velocity (speed and direction) starting at 14:00 hours on 14. August 2016 and ending at 17:00 hours on 20. May 2017. The temperature data are all considered good whereas some of the ADCP velocities have been flagged. The interpolation procedures increased the original percentage of good (non-flagged) velocity values considerably (column 5 in Table 3). Table 3 also lists the average (residual) velocity (speed and direction) for each bin for all good hourly records.

From the original quality controlled ADCP data (20 minute interval), the main tidal constituents were determined. For the whole water column, the tidal current is semi-diurnal, dominated by the M2 constituent. In Appendix A, details of the tidal current velocities for each bin are listed for the five most significant constituents (three semi-diurnal and two diurnal).

Based on the hourly temperature values, we computed daily averaged temperatures for each of the three sites by averaging the 25 (to reduce tidal influence) hourly values from 00:00 hours to 24:00 hours every day from 15. August 2016 to 19. May 2017.

Table 3. Details of the ADCP measurements. The instrument was and RDI 150 kHz Broadband ADCP, serial number 1279. Below are for each bin shown the height over bottom and depth of the centre of the bin, the original (20 minute interval) and final (interpolated hourly interval) percentage of good (non-flagged) values, and speed and direction of the residual current based on hourly averaged good data for all records.

Bin	Height	Depth	Good data		Residual	
			Orig.	Final	Speed	Dir
	(m)	(m)	(%)	(%)	(cm/s)	(°)
1	17	385	99.53	99.90	4.9	207
2	27	375	99.34	99.99	4.2	212
3	37	365	99.15	100.00	2.9	216
4	47	355	99.11	100.00	1.5	213
5	57	345	99.03	99.99	0.6	123
6	67	335	99.01	100.00	2.0	80
7	77	325	98.79	99.97	3.5	75
8	87	315	98.68	99.99	4.9	73
9	97	305	98.65	100.00	6.2	72
10	107	295	98.60	99.99	7.4	71
11	117	285	98.56	99.99	8.6	70
12	127	275	98.51	99.99	9.7	69
13	137	265	98.32	99.93	10.8	69
14	147	255	98.22	99.85	12.0	69
15	157	245	98.16	99.84	13.0	70
16	167	235	97.89	99.72	14.0	70
17	177	225	97.39	99.42	14.9	71
18	187	215	96.81	98.97	15.7	71
19	197	205	96.38	98.15	16.4	71
20	207	195	95.59	97.39	17.1	72
21	217	185	93.96	95.91	17.7	73
22	227	175	92.42	94.10	18.2	74
23	237	165	90.03	92.28	18.8	74
24	247	155	87.59	89.93	19.3	75
25	257	145	84.78	87.07	20.0	75
26	267	135	79.34	81.99	20.1	75
27	277	125	73.10	75.69	20.3	76
28	287	115	65.37	67.85	20.2	77
29	297	105	57.20	59.63	20.2	78
30	307	95	49.00	49.90	20.5	79

Daily averaged velocity profiles were computed by a standard package, which involves de-tiding of the velocity before averaging. This reduces biasing by tides in time series with gaps and the percentage of good data increase considerably, so that the daily average velocities were 100% good up to bin 26 (267 m above the bottom) as indicated in Table 4. This is especially important since the tidal velocities are generally stronger than the residual velocities, especially for the bottom-near bins (Table 4).

The typical current directions for various depths at site B are illustrated in Figure 6. For six selected bins, the figure shows the average velocity in 15° directional classes. For bin 1, centred 17 m above the bottom, the average velocity is strongest towards the southwest; roughly following the axis of the Western Valley in the direction where we would expect overflow to occur. Fifty meter higher up in the water column, bin 6 has the strongest flow in almost the opposite direction, indicating that the Atlantic inflow towards the Norwegian Sea dominates. As we progress upwards, this tendency increases and for bin 26, the flow is almost uni-directional into the Norwegian Sea (Figure 6).

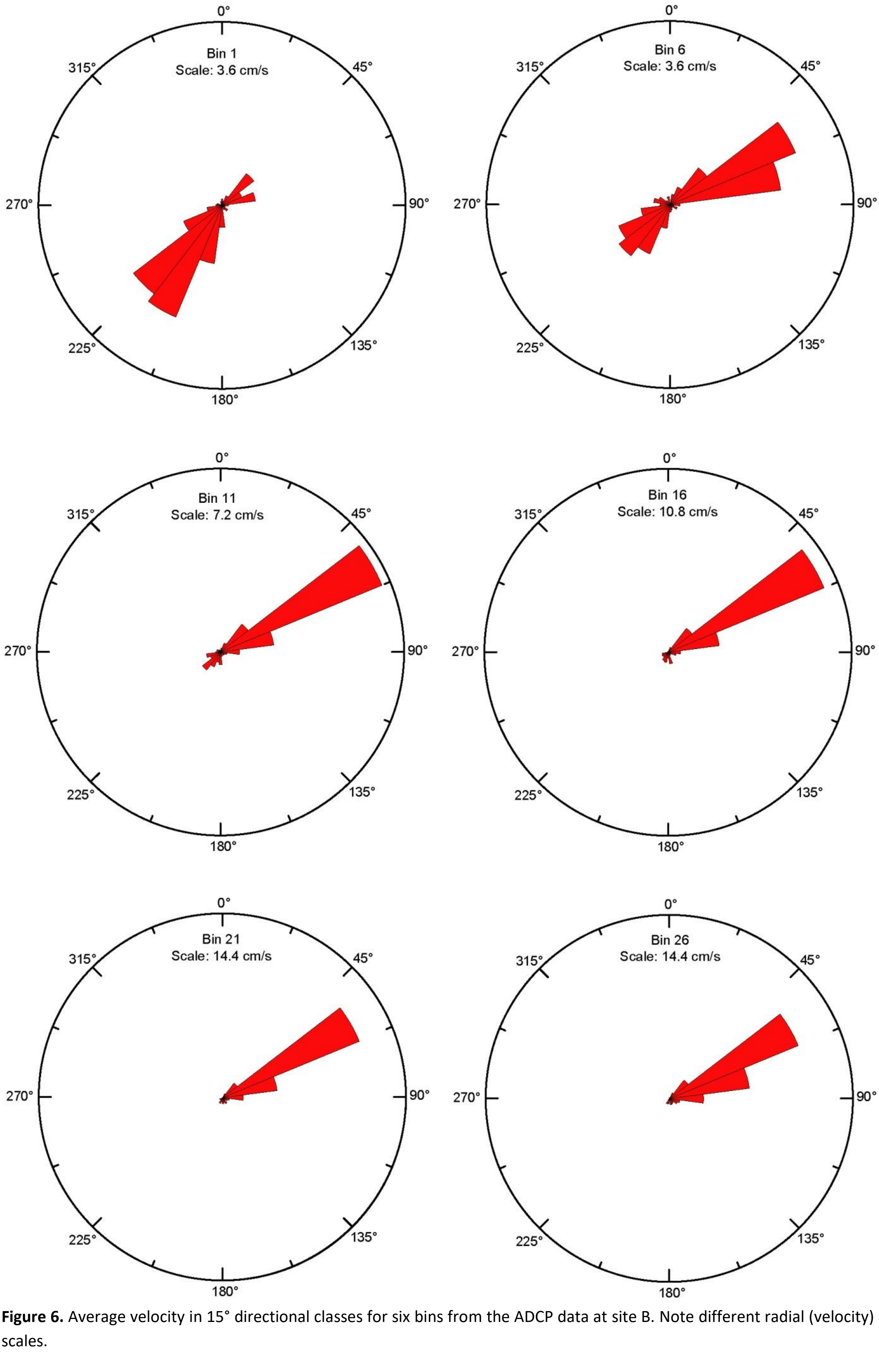

Figure 6. Average velocity in 15° directional classes for six bins from the ADCP data at site B. Note different radial (velocity) scales.

Table 4. Residual velocity (speed and direction) of the daily averaged ADCP data, percentage good (non-flagged) daily average values, major and minor semi-axes of the M2 tidal ellipse.

			Daily averaged			M2 tidal ellipse	
Bin	Hgth (m)	Depth (m)	Speed (cm/s)	Dir (°)	Good (%)	Major (cm/s)	Minor (cm/s)
1	17	385	4.9	208	100.0	16.5	6.4
2	27	375	4.2	212	100.0	18.0	4.8
3	37	365	3.0	216	100.0	19.7	2.7
4	47	355	1.6	215	100.0	21.4	0.6
5	57	345	0.6	140	100.0	23.1	1.4
6	67	335	1.9	83	100.0	24.6	3.1
7	77	325	3.4	77	100.0	26.0	4.7
8	87	315	4.9	76	100.0	27.3	6.1
9	97	305	6.2	74	100.0	28.6	7.5
10	107	295	7.4	73	100.0	29.7	8.6
11	117	285	8.6	71	100.0	30.7	9.4
12	127	275	9.7	70	100.0	31.5	10.2
13	137	265	10.8	70	100.0	32.2	11.0
14	147	255	11.9	70	100.0	33.1	11.6
15	157	245	13.0	71	100.0	34.0	12.4
16	167	235	14.0	71	100.0	34.9	13.1
17	177	225	14.9	71	100.0	35.9	13.7
18	187	215	15.8	72	100.0	36.7	14.4
19	197	205	16.7	72	100.0	37.4	14.9
20	207	195	17.5	72	100.0	37.8	15.3
21	217	185	18.4	73	100.0	38.2	15.6
22	227	175	19.2	73	100.0	38.4	15.9
23	237	165	20.0	73	100.0	38.8	16.3
24	247	155	20.9	73	100.0	39.3	16.5
25	257	145	21.6	72	100.0	39.6	16.7
26	267	135	22.1	73	100.0	39.7	16.9
27	277	125	22.6	73	99.6	40.3	17.0
28	287	115	22.4	74	96.8	40.7	16.8
29	297	105	21.8	75	92.1	41.8	16.6
30	307	95	20.9	77	86.3	41.5	16.4

CTD data

The CTD data from the deployment cruise as well as from the recovery cruise have been quality controlled and calibrated and are stored together with the collected historical CTD data in the database generated for the WOW project.

Appendix A

Frequency (in parts per thousand) of speeds equal to or exceeding specified vales for the ADCP at site B.

Bin no.	Depth m	Speed (cm/s) 10	20	30	40	50	60	70	80	90	100	110	120	130	140	150	160	170	180
1	385	821	440	172	53	18	6	2	1	0	0	0	0	0	0	0	0	0	0
2	375	810	456	201	75	27	11	4	2	1	0	0	0	0	0	0	0	0	0
3	365	798	463	218	88	36	16	7	3	1	0	0	0	0	0	0	0	0	0
4	355	796	478	239	102	45	21	9	5	2	1	0	0	0	0	0	0	0	0
5	345	805	496	254	122	54	25	12	6	3	1	0	0	0	0	0	0	0	0
6	335	819	517	279	136	67	31	14	7	3	0	0	0	0	0	0	0	0	0
7	325	835	539	305	155	80	40	18	8	4	1	0	0	0	0	0	0	0	0
8	315	855	573	328	175	94	50	25	11	4	1	0	0	0	0	0	0	0	0
9	305	864	600	353	197	108	60	32	14	5	1	0	0	0	0	0	0	0	0
10	295	879	628	378	218	119	71	41	19	7	2	0	0	0	0	0	0	0	0
11	285	885	649	405	238	134	80	47	24	10	2	1	0	0	0	0	0	0	0
12	275	891	667	428	256	147	88	53	30	13	3	1	0	0	0	0	0	0	0
13	265	895	681	448	274	160	96	59	34	15	4	1	0	0	0	0	0	0	0
14	255	898	692	469	295	175	105	66	39	19	6	1	0	0	0	0	0	0	0
15	245	905	707	488	311	189	114	71	44	23	8	2	0	0	0	0	0	0	0
16	235	904	720	506	327	201	124	78	48	25	10	2	0	0	0	0	0	0	0
17	225	909	727	522	342	213	131	83	52	29	12	3	0	0	0	0	0	0	0
18	215	905	735	533	358	226	138	86	53	29	12	3	1	0	0	0	0	0	0
19	205	902	743	542	366	235	146	91	55	30	12	3	1	0	0	0	0	0	0
20	195	898	746	548	373	238	148	93	57	29	12	4	0	0	0	0	0	0	0
21	185	885	741	553	373	243	149	92	55	29	12	4	1	0	0	0	0	0	0
22	175	874	736	554	379	242	151	94	56	28	12	4	1	0	0	0	0	0	0
23	165	855	726	550	375	242	151	92	55	28	12	4	1	0	0	0	0	0	0
24	155	834	714	547	378	242	148	91	53	27	12	5	1	0	0	0	0	0	0
25	145	809	700	537	376	241	148	89	52	26	12	5	1	0	0	0	0	0	0
26	135	758	659	507	356	229	141	85	49	24	10	4	1	0	0	0	0	0	0
27	125	701	609	474	334	218	134	81	47	23	11	5	1	0	0	0	0	0	0
28	115	627	548	427	303	195	120	74	43	21	9	4	1	0	0	0	0	0	0
29	105	550	481	375	266	175	106	65	39	19	9	4	1	0	0	0	0	0	0
30	95	471	417	326	232	153	94	58	35	18	8	3	1	0	0	0	0	0	0

The following three pages contain five tables with data for the constituents M2, S2, N2, O1, and K1, computed by an adapted version of the Foreman FORTRAN package. Each table lists for each bin the amplitude and Greenwich phase lag for the east and north velocity components and lists also major and minor semi-axes of the tidal ellipse for the constituent as well as its inclination, Greenwich phase lag (Figure A1), and sense of rotation (cyclonic = C, anticyclonic = A).

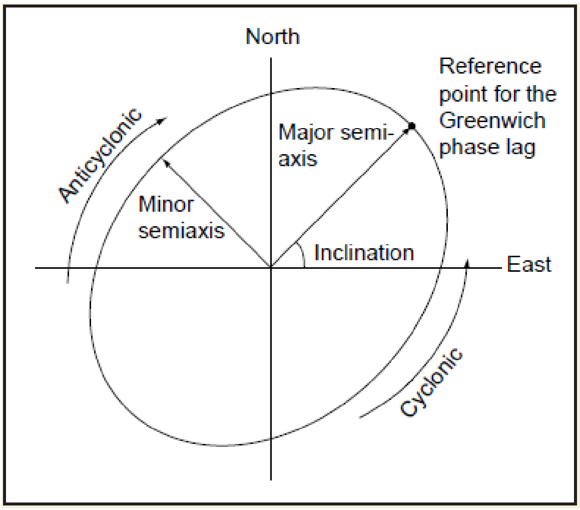

Figure A1. Parameters of the tidal ellipse for a given constituent. The reference point for the Greenwich phase lag is always chosen to be above the east-west axis.

Harmonic constants for constituent M2 at site B.

Bin	Depth m	E-ampl mm/sec	E-gpl deg	N-ampl mm/sec	N-gpl deg	Major mm/sec	Minor mm/sec	Incl deg	Grphl deg	R
01	385	154	209	88	260	165	64	23	218	C
02	375	159	216	97	250	180	48	29	225	C
03	365	163	225	113	241	197	27	34	230	C
04	355	169	232	132	236	214	6	38	234	C
05	345	177	239	150	232	231	14	40	236	A
06	335	186	244	164	230	246	31	41	238	A
07	325	195	248	178	228	260	47	42	239	A
08	315	204	252	191	227	273	61	43	240	A
09	305	213	255	204	226	286	75	44	241	A
10	295	220	258	217	226	297	86	45	242	A
11	285	227	260	227	226	307	94	45	243	A
12	275	232	262	237	226	315	102	46	244	A
13	265	236	264	246	227	322	110	46	244	A
14	255	240	266	256	227	331	116	47	245	A
15	245	246	269	266	228	340	124	48	247	A
16	235	252	271	275	229	349	131	48	248	A
17	225	258	272	284	230	359	137	49	249	A
18	215	264	274	293	231	367	144	49	249	A
19	205	268	275	300	231	374	149	49	250	A
20	195	270	276	306	231	378	153	50	250	A
21	185	272	276	310	231	382	156	50	250	A
22	175	274	277	314	231	384	159	51	250	A
23	165	278	278	316	232	388	163	50	251	A
24	155	281	278	320	231	393	165	50	251	A
25	145	284	278	323	231	396	167	50	251	A
26	135	285	278	323	231	397	169	50	251	A
27	125	287	277	330	231	403	170	51	250	A
28	115	290	277	331	231	407	168	50	250	A
29	105	299	276	336	232	418	166	50	251	A
30	95	296	276	334	232	415	164	50	251	A

Harmonic constants for constituent S2 at site B.

Bin	Depth m	E-ampl mm/sec	E-gpl deg	N-ampl mm/sec	N-gpl deg	Major mm/sec	Minor mm/sec	Incl deg	Grphl deg	R
01	385	71	257	36	275	79	10	26	261	C
02	375	75	264	42	268	87	3	29	265	C
03	365	76	270	50	268	91	1	33	269	A
04	355	74	274	55	268	92	4	36	272	A
05	345	73	278	60	268	94	8	39	274	A
06	335	73	283	64	267	97	13	41	276	A
07	325	75	286	70	265	101	18	43	277	A
08	315	78	289	76	263	106	24	44	277	A
09	305	80	291	81	262	110	28	45	277	A
10	295	82	293	85	263	114	31	46	277	A
11	285	84	295	90	264	119	33	47	279	A
12	275	85	298	94	266	122	35	48	280	A
13	265	86	300	97	267	125	37	49	281	A
14	255	88	302	100	268	128	38	49	282	A
15	245	89	304	102	269	129	41	50	284	A
16	235	90	307	104	270	131	43	50	285	A
17	225	91	309	107	271	134	44	51	287	A
18	215	91	311	110	272	135	47	52	287	A
19	205	92	312	113	273	137	48	53	288	A
20	195	92	314	115	273	139	50	53	288	A
21	185	91	314	118	273	140	50	55	287	A
22	175	94	314	120	274	143	50	54	288	A
23	165	95	315	120	274	144	52	54	289	A
24	155	97	315	121	274	145	54	53	289	A
25	145	97	317	120	273	144	56	53	290	A
26	135	96	316	119	273	142	55	53	289	A
27	125	101	318	117	273	143	58	51	291	A
28	115	105	319	116	273	144	61	49	293	A
29	105	102	320	118	275	144	60	51	293	A
30	95	106	323	116	274	144	65	49	296	A

Harmonic constants for constituent N2 at site B.

Bin	Depth m	E-ampl mm/sec	E-gpl deg	N-ampl mm/sec	N-gpl deg	Major mm/sec	Minor mm/sec	Incl deg	Grphl deg	R
01	385	26	195	26	255	32	18	43	224	C
02	375	27	207	28	249	36	14	46	228	C
03	365	29	221	31	239	42	7	47	230	C
04	355	33	229	33	227	47	1	45	228	A
05	345	40	231	36	216	53	7	42	224	A
06	335	46	230	38	206	59	12	39	221	A
07	325	50	229	41	200	63	16	38	218	A
08	315	53	229	42	197	65	18	38	217	A
09	305	54	228	44	194	67	20	38	215	A
10	295	53	230	45	194	67	21	39	215	A
11	285	54	231	47	193	68	23	41	215	A
12	275	54	234	50	195	69	24	42	216	A
13	265	54	238	52	197	70	26	44	219	A
14	255	55	242	55	198	72	29	45	220	A
15	245	57	245	57	198	74	32	45	222	A
16	235	58	247	59	199	76	34	46	222	A
17	225	59	247	60	198	77	35	46	222	A
18	215	60	248	61	199	78	36	45	223	A
19	205	61	249	62	201	80	36	45	225	A
20	195	61	251	63	203	80	36	47	226	A
21	185	62	252	66	204	83	37	47	226	A
22	175	60	256	67	206	81	38	50	227	A
23	165	61	260	67	209	82	39	50	231	A
24	155	59	258	68	208	82	38	51	228	A
25	145	58	260	67	209	80	38	52	229	A
26	135	57	259	66	210	79	35	51	230	A
27	125	56	260	64	212	78	35	51	231	A
28	115	50	255	65	209	76	31	55	225	A
29	105	50	254	66	209	77	31	56	224	A
30	95	42	256	62	202	68	31	62	215	A

Harmonic constants for constituent O1 at site B.

Bin	Depth m	E-ampl mm/sec	E-gpl deg	N-ampl mm/sec	N-gpl deg	Major mm/sec	Minor mm/sec	Incl deg	Grphl deg	R
01	385	29	346	23	29	35	13	36	2	C
02	375	32	349	22	28	37	12	32	0	C
03	365	34	348	18	25	37	10	25	356	C
04	355	33	347	15	23	35	8	21	352	C
05	345	31	344	11	20	33	6	17	347	C
06	335	30	342	8	17	31	4	12	344	C
07	325	30	337	6	18	30	4	9	338	C
08	315	28	333	5	28	29	4	5	333	C
09	305	28	324	2	63	28	2	179	144	C
10	295	28	317	1	131	28	0	177	137	C
11	285	30	313	3	178	30	2	176	133	A
12	275	31	307	6	190	31	5	175	128	A
13	265	31	305	7	193	31	7	175	126	A
14	255	30	303	10	192	30	9	173	125	A
15	245	29	301	11	188	29	10	170	124	A
16	235	30	296	13	192	30	12	173	118	A
17	225	30	293	12	194	30	11	176	114	A
18	215	30	291	13	194	30	12	176	112	A
19	205	32	290	15	195	32	15	177	112	A
20	195	34	288	16	195	34	16	178	109	A
21	185	35	285	18	192	35	18	179	105	A
22	175	34	280	21	186	34	21	176	102	A
23	165	34	276	23	187	34	23	2	274	A
24	155	34	284	22	189	34	21	175	107	A
25	145	34	281	22	189	34	22	177	103	A
26	135	35	294	19	189	36	18	169	119	A
27	125	36	294	21	192	36	20	170	119	A
28	115	41	304	17	198	42	16	172	127	A
29	105	38	324	12	178	39	6	165	147	A
30	95	49	326	7	185	50	4	174	147	A

Harmonic constants for constituent K1 at site B.

Bin	Depth m	E-ampl mm/sec	E-gpl deg	N-ampl mm/sec	N-gpl deg	Major mm/sec	Minor mm/sec	Incl deg	Grphl deg	R
01	385	33	264	19	312	36	13	25	274	C
02	375	36	266	18	312	38	12	21	273	C
03	365	37	266	14	308	39	9	17	270	C
04	355	38	263	11	299	39	6	13	265	C
05	345	37	260	7	283	38	3	10	261	C
06	335	38	255	4	267	38	1	7	255	C
07	325	37	249	4	231	37	1	5	249	A
08	315	36	245	4	204	36	3	5	244	A
09	305	36	241	5	186	36	4	5	240	A
10	295	36	238	7	164	36	7	3	237	A
11	285	36	233	10	157	36	10	4	232	A
12	275	37	229	12	141	37	12	1	229	A
13	265	37	226	13	136	37	13	0	226	A
14	255	38	223	15	130	38	15	179	43	A
15	245	39	221	16	122	39	16	175	43	A
16	235	38	221	18	120	38	17	173	44	A
17	225	36	222	18	116	37	17	170	47	A
18	215	34	223	20	115	35	19	166	51	A
19	205	34	222	21	114	34	19	165	50	A
20	195	33	219	22	113	34	20	163	50	A
21	185	29	211	23	108	30	22	159	47	A
22	175	28	201	25	108	28	25	165	34	A
23	165	28	197	27	108	28	27	12	185	A
24	155	27	197	29	108	29	27	85	113	A
25	145	28	201	30	111	30	28	92	109	A
26	135	30	207	27	108	32	26	153	50	A
27	125	35	207	28	115	35	28	176	30	A
28	115	41	215	24	114	42	24	171	40	A
29	105	36	215	26	102	38	22	154	51	A
30	95	52	223	25	104	53	21	164	50	A

P.O. Box 3051 · Nóatún 1
FO-110 Tórshavn
Faroe Islands

Tel +298 35 39 00
hav@hav.fo
www.hav.fo